Available online at www.sciencedirect.com

ScienceDirect

IFAC Papers Online CONFERENCE PAPER ARCHIVE

IFAC PapersOnLine 51-30 (2018) 548–553

Force control design for a robot manipulator attached to a UAV

Konstantinos Gkountas *, **Dimitris Chaikalis** *, and **Anthony Tzes** **

* *University of Patras, Electrical and Computer Engineering Department, Rio 26500, Greece (e-mail:gkountas@ece.upatras.gr, ece8560@upnet.gr).*

** *New York University Abu Dhabi, Electrical and Computer Engineering, Abu Dhabi 129188, United Arab Emirates (e-mail: anthony.tzes@nyu.edu)*

Abstract: This article focuses on the modeling and control of an Unmanned Aerial Vehicle (UAV) while applying forces to its surrounding environment using a manipulator. The manipulator is attached beneath the UAV. The derived mathematical model of the UAV carrying the manipulator, relies on the application of the Newton-Euler equations. Model-based controllers are designed, in order to stabilize the UAV while maintaining the contact with its surrounding environment and applying forces to it. The objective is to keep the end effector of the manipulator as close as possible to a desired point while at the same time exerting forces to it. Simulation studies using a quadrotor and a two Degree of Freedom (DoF) planar manipulator are provided to demonstrate the effectiveness of the proposed control scheme.

Keywords: Unmanned Aerial Systems, Floating base Manipulator, Force Control

1. INTRODUCTION

The rapid growth of the UAVs in the last decade has led to an increment in the demand of the services that they can provide. Although, these systems are already used in a wide variety of applications including wildfire surveillance over forest areas (Pham et al., 2017), search and rescue, buildings inspection filming and open area mapping (Sujit et al., 2014), they lack the capability of interacting with their surroundings. Performing interaction activities is being highly investigated, leading to new opportunities in the applications that UAVs can provide (Wopereis et al., 2017).

Inspired by this new trend, many researchers are focused in the physical interaction of UAVs with their environment (Marconi et al., 2011). In order to achieve such an activity, UAVs are equipped with ropes (Pereira and Dimarogonas, 2017) or robotic manipulators (Kamel et al., 2016). UAVs equipped with manipulators, referred to as aerial manipulators, are usually prefered as they offer more precise and elegant movements (Ruggiero et al., 2018).

UAVs can be used to improve the conditions in remoted regions where they can carry equipment or medical devices in non- accessible by human areas. Moreover, by developing more accurate models and controllers, UAVs can perform more dangerous tasks interacting with humans, improving workplace safety.

The modeling of a UAV with an attached robotic manipulator is an extremely complicated problem. The mathematical model that describes such a system is nonlinear and very complex due to the fact that the maneuvers of the UAV affect the manipulator while the movement of the manipulator has an impact on the UAV stability. The dynamic model becomes even more complex by integrating the forces and the torques that may be applied to the tip of the manipulator.

In this paper, we consider a UAV with an attached 2 DoF manipulator while it is applying forces to its environment. The trivial equations for a UAV are used, combined with the recursive Newton-Euler equations for the manipulator in order to take into account the moving base of the manipulator and the forces at the end of the manipulator. The derived dynamic model is used to simulate the coupled system and provides us the opportunity to build model-based control methods concerning the interaction of the system with its environment by the way of forces applied by the manipulator.

The remainder of this paper is organized as follows: In Section 2 we establish the mathematical models of the UAV and the manipulator. In Section 3, control schemes for both the UAV and the manipulator are developed. Finally, in Section 4, simulation studies ran on the Gazebo simulator are presented validating our approach and showing the efficiency of our controllers.

2. SYSTEM MODELING

Our system consists of two individual subsystems, the UAV and the robotic manipulator, as shown in Fig. 1. The recursive Newton-Euler (N-E) formulation is employed for deriving the system dynamics.

2405-8963
10.1016/j.ifacol.2018.11.268

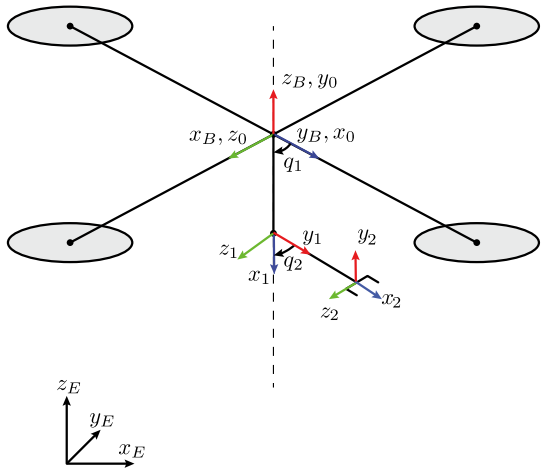

Fig. 1. UAV system equipped with a 2 DoF robotic manipulator

2.1 UAV Dynamics

Let us consider our UAV to be a symmetrical quadrotor, where we introduce the vehicle frame which is located on the UAV and coincides with the quadrotor's center of mass as the Body-Fixed Frame (B-frame) and the inertial coordinate system which is an Earth-Fixed Frame (E-frame). The orthonormal rotation matrix that allows us to transform a vector in B-frame to E-frame is defined as

$$ {}^{E}R_{B} = \begin{bmatrix} c\theta c\psi & s\phi s\theta c\psi - c\phi s\psi & c\phi s\theta c\psi + s\phi s\psi \\ c\theta s\psi & s\phi s\theta s\psi + c\phi c\psi & c\phi s\theta s\psi - s\phi c\psi \\ -s\theta & s\phi c\theta & c\phi c\theta \end{bmatrix}, $$

$$ {}^{B}R_{E} = {}^{E}R_{B}{}^{\top} $$

The dynamic equations of the UAV, are derived based on the Newton-Euler method, where

$$ \begin{bmatrix} m_s \mathrm{I}_{3\times3} & \mathrm{O}_{3\times3} \\ \mathrm{O}_{3\times3} & I \end{bmatrix} \begin{bmatrix} \dot{V} \\ \dot{\omega} \end{bmatrix} + \begin{bmatrix} \omega \times V \\ \omega \times I\omega \end{bmatrix} = \begin{bmatrix} F \\ \tau \end{bmatrix}, \quad (1) $$

where m_s denotes the mass of the UAV, $\mathrm{I}_{3\times3}$ and $\mathrm{O}_{3\times3}$ are the identity matrix and the zero matrix, respectively. I corresponds to the moment of inertia around the center of mass of the body, V represents the translational velocity while ω represents the angular velocity of the body. Finally, F and τ denote the total force and torque vectors acting on the center of mass of the body

According to (Alexis et al., 2012), omitting hub forces, the friction forces, the rolling moments and the external disturbances a UAV can be described by the simplified nonlinear differential equations

$$ \begin{bmatrix} \dot{V}_E \\ \dot{\omega}_B \end{bmatrix} = \begin{bmatrix} \ddot{x} \\ \ddot{y} \\ \ddot{z} \\ \ddot{\phi} \\ \ddot{\theta} \\ \ddot{\psi} \end{bmatrix} = \begin{bmatrix} u_x U_1/m_s \\ u_y U_1/m_s \\ -g + (c\phi c\theta)U_1/m_s \\ \dot{\theta}\dot{\psi}a_1 + b_1 U_2 \\ \dot{\phi}\dot{\psi}a_2 + b_2 U_3 \\ \dot{\theta}\dot{\phi}a_3 + b_3 U_4 \end{bmatrix}, \text{ where} \quad (2) $$

$$ u_x = c\phi s\theta c\psi + s\phi s\psi, \quad u_y = c\phi s\theta s\psi + s\phi c\psi \quad (3) $$

$$ a_1 = (I_{yy} - I_{zz})/I_{xx}, \quad a_2 = (I_{zz} - I_{xx})/I_{yy} \quad (4) $$

$$ a_3 = (I_{xx} - I_{yy})/I_{zz} \quad (5) $$

$$ b_1 = l_a/I_{xx}, \quad b_2 = l_a/I_{yy}, \quad b_3 = 1/I_{zz}. \quad (6) $$

where $\dot{V}_E = [\ddot{x},\ \ddot{y},\ \ddot{z}]^{\top}$ is the translational acceleration expressed in the E-frame and $\dot{\omega}_B = [\ddot{\phi},\ \ddot{\theta},\ \ddot{\psi}]^{\top}$ is the angular acceleration expressed in the B-frame. Parameters u_x and u_y represent the directions of thrust vector that cause the motion about the E_x and E_y axis respectively and U_1, in combination with ϕ and θ states, rule the altitude motion. Assuming the thrust and drag forces are proportional to the square of the angular speed of the rotors, we define the fictitious control inputs $U_i \in \Re,\ i = 1, \ldots, 4$ as

$$ \begin{bmatrix} U_1 \\ U_2 \\ U_3 \\ U_4 \end{bmatrix} = \begin{bmatrix} b(\Omega_1^2 + \Omega_2^2 + \Omega_3^2 + \Omega_4^2) \\ b(-\Omega_2^2 + \Omega_4^2) \\ b(\Omega_1^2 - \Omega_3^2) \\ d(-\Omega_1^2 + \Omega_2^2 - \Omega_3^2 + \Omega_4^2) \end{bmatrix} \quad (7) $$

The input U_1 is related to the total thrust, the inputs U_2, U_3 and U_4 are related to the rotations of the UAV, $\Omega_i,\ i = 1, \ldots, 4 \in \Re^{+}$ are the rotational speeds of the propellers, m_s is the total mass of the UAV and $g = 9.81\ [m/s^2]$ is the gravitational acceleration. The rest of the parameters involved in equations 6-7 are listed in Table 1.

Table 1. Parameter table

I_{xx}	Moment of inertia of the UAV about the B_x axis
I_{yy}	Moment of inertia of the UAV about the B_y axis.
I_{zz}	Moment of inertia of the UAV about the B_z axis.
l_a	Arm length of the UAV.
b	Thrust coefficient.
d	Drag coefficient.

2.2 Floating base manipulator dynamics

In the case of the floating base manipulator, the recursive N-E method (RNE) is employed since:a) the position, b) the orientation of the Base-Fixed Frame, and c) the representation of the gravity vector vary as the UAV moves. The RNE method uses a set of forward and backward recursions (Fu et al., 1987). The forward recursion is used to propagate the velocities and accelerations from one link to the next. These linear and angular velocities and accelerations computed are in turn used in the backward recursion to calculate the forces and torques exerted on each link. In this article, all parameters are referenced to their own link coordinate frames, resulting in a computation time proportional to the number of the manipulator's joints.

(1) Forward Recursion: Here the angular and linear velocities and accelerations of each link are calculated recursively in terms of its preceding link starting from the base to the end-effector. The initial conditions for the base link are $v_0 = v$, $\dot{v}_0 = \dot{v}$ and $\omega_0 = \Omega$, $\dot{\omega}_0 = \dot{\Omega}$. With these initializations the "forward" equations are calculated for $i = 1, 2, \ldots, n$ as

if joint i is rotational

$$ {}^{i}R_0\omega_i = {}^{i}R_{i-1}\left({}^{i-1}R_0\omega_{i-1} + z_0\dot{q}_i\right) $$

$$ {}^{i}R_0\dot{\omega}_i = {}^{i}R_{i-1}\left({}^{i-1}R_0\dot{\omega}_{i-1} + z_0\ddot{q}_i + \left({}^{i-1}R_0\omega_{i-1}\right) \times z_0\dot{q}_i\right) $$

$$ {}^{i}R_0\dot{v}_i = \left({}^{i}R_0\dot{\omega}_i\right) \times \left({}^{i}R_0p_i^*\right) + \left({}^{i}R_0\omega_i\right) \times \left(\left({}^{i}R_0\omega_i\right) \times \left({}^{i}R_0p_i^*\right)\right) + {}^{i}R_{i-1}\left({}^{i-1}R_0\dot{v}_{i-1}\right) $$

$$
\begin{aligned}
{}^{i}R_0\bar{a}_i = {} & \left({}^{i}R_0\dot{\omega}_i\right) \times \left({}^{i}R_0\bar{s}_i\right) + \left({}^{i}R_0\omega_i\right) \times \left(\left({}^{i}R_0\omega_i\right) \times \left({}^{i}R_0\bar{s}_i\right)\right) \\
& + {}^{i}R_0\dot{v}_i
\end{aligned}
$$

if joint i is translational

$$
\begin{aligned}
{}^{i}R_0\omega_i &= {}^{i}R_{i-1}\left({}^{i-1}R_0\omega_{i-1}\right) \\
{}^{i}R_0\dot{\omega}_i &= {}^{i}R_{i-1}\left({}^{i-1}R_0\dot{\omega}_{i-1}\right) \\
{}^{i}R_0\dot{v}_i &= {}^{i}R_{i-1}\left(z_0\ddot{q}_i + {}^{i-1}R_0\dot{v}_{i-1}\right) + \left({}^{i}R_0\dot{\omega}_i\right) \times \left({}^{i}R_0p_i^*\right) \\
&\quad + 2\left({}^{i}R_0\omega_i\right) \times \left({}^{i}R_{i-1}z_0\dot{q}_i\right) \\
&\quad + \left({}^{i}R_0\omega_i\right) \times \left(\left({}^{i}R_0\omega_i\right) \times \left({}^{i}R_0p_i^*\right)\right) \\
{}^{i}R_0\bar{a}_i &= \left({}^{i}R_0\dot{\omega}_i\right) \times \left({}^{i}R_0\bar{s}_i\right) + \left({}^{i}R_0\omega_i\right) \times \left(\left({}^{i}R_0\omega_i\right) \times \left({}^{i}R_0\bar{s}_i\right)\right) \\
&\quad + {}^{i}R_0\dot{v}_i
\end{aligned}
$$

where $\bar{s}_i$ is the position of the center of mass of link i from the origin of the i-th local coordinate system, p_i^* is the origin of the i-th coordinate frame with respect to the the $(i-1)$-th coordinate system, ω_i is the angular velocity of link i, v_i is the linear velocity of the center of mass of link i, $\bar{a}_i$ is the linear acceleration of the center of mass of link i, q_i denotes the joint variable of link i and $z_0 = [0,0,1]^\top$.

(2) Backward Recursion: After the velocities and accelerations of the links are computed, the joint forces may be computed for each link starting from the end-effector to the base. The required "backward" equations are calculated for $i = n, n-1, \ldots, 1$ as:

if joint i is rotational

$$
\begin{aligned}
{}^{i}R_0f_i &= {}^{i}R_{i+1}\left({}^{i+1}R_0f_{i+1}\right) + m_i{}^{i}R_0\bar{a}_i \\
{}^{i}R_0\eta_i &= {}^{i}R_{i+1}\left({}^{i+1}R_0\eta_{i+1} + \left({}^{i+1}R_0p_i^*\right) \times \left({}^{i+1}R_0f_{i+1}\right)\right) \\
&\quad + \left({}^{i}R_0p_i^* + {}^{i}R_0\bar{s}_i\right) \times \left({}^{i}R_0F_i\right) \\
&\quad + \left({}^{i}R_0{I_i}^0R_i\right)\left({}^{i}R_0\dot{\omega}_i\right) \\
&\quad + \left({}^{i}R_0\omega_i\right) \times \left(\left({}^{i}R_0{I_i}^0R_i\right)\left({}^{i}R_0\omega_i\right)\right) \\
\tau_i &= \left({}^{i}R_0\eta_i\right)^\top \left({}^{i}R_{i-1}z_0\right) + b_i\dot{q}_i
\end{aligned} \tag{8}
$$

if joint i is translational

$$
\begin{aligned}
{}^{i}R_0f_i &= {}^{i}R_{i+1}\left({}^{i+1}R_0f_{i+1}\right) + m_i{}^{i}R_0\bar{a}_i \\
{}^{i}R_0\eta_i &= {}^{i}R_{i+1}\left({}^{i+1}R_0\eta_{i+1} + \left({}^{i+1}R_0p_i^*\right) \times \left({}^{i+1}R_0f_{i+1}\right)\right) \\
&\quad + \left({}^{i}R_0p_i^* + {}^{i}R_0\bar{s}_i\right) \times \left({}^{i}R_0F_i\right) \\
&\quad + \left({}^{i}R_0{I_i}^0R_i\right)\left({}^{i}R_0\dot{\omega}_i\right) \\
&\quad + \left({}^{i}R_0\omega_i\right) \times \left(\left({}^{i}R_0{I_i}^0R_i\right)\left({}^{i}R_0\omega_i\right)\right) \\
\tau_i &= \left({}^{i}R_0f_i\right)^\top \left({}^{i}R_{i-1}z_0\right) + b_i\dot{q}_i
\end{aligned} \tag{9}
$$

where m_i is the total mass of link i, $F_i = m_i\bar{a}_i$ is the total external force exerted on link i at the center of mass, I_i is the inertia matrix of link i about its center of mass with reference to the O-frame, f_i is the force exerted on link i by link $i-1$ at the $(i-1)$-th local coordinate frame to support link i and the links above it, η_i is the moment exerted on link i by link $i-1$ at the $(i-1)$-th local coordinate frame and b_i is the viscous damping coefficient for joint i. For the remainder of this work we neglect the damping effects and we assume that $b_i = 0$ for all $i = 1, \ldots, n$. The backward recursion initial conditions are determined according to the load affecting the manipulator's end-effector. In the above equations, ${}^{i}R_{i-1}$ denotes the orthogonal rotation matrix used to transform a vector from frame $i-1$ to frame i.

If both recursions are executed symbolically then equations (8), (9) provide a closed-form expression for the dynamics of an n-link manipulator, as

$$
D(q)\ddot{q} + C(q,\dot{q})\dot{q} + G(q) = \tau, \tag{10}
$$

where $q \in \Re^n$ is the vector of joint variables, $D(q) \in \Re^{n\times n}$ is the generalized inertia matrix, $C(q) \in \Re^n$ is the Coriolis matrix, $G(q) = [g_1(q), \ldots, g_n(q)]^\top$ is the gravity vector and $\tau = [\tau_1, \ldots, \tau_n]^\top$ is the vector of generalized forces; that is, the i-th element denotes either the force or the torque applied to the i-th joint of the manipulator.

2.3 Coupled UAV/Manipulator System Dynamics

In order to derive the dynamics of the entire system, we shall combine the dynamic models of the subsystems it consists of, as described in (Stergiopoulos et al., 2016). The computation of the RNE equations provides us with the forces and torques, that are applied on the center of mass of the UAV due to the manipulator. However, utilizing the Recursive Newton-Euler equations, we can add a fictional force at the end of the last link of the manipulator and compute symbolically the reactions that can be observed on the UAV. Thus, we derive the dynamic model of our system including the forces applied at the end effector.

The manipulator configuration with respect to the other (UAV and inertial) frames is

$$
{}^{O}R_E = {}^{O}R_B{}^{B}R_E, \quad {}^{O}R_B = \begin{bmatrix} 0 & 1 & 0 \\ 0 & 0 & 1 \\ 1 & 0 & 0 \end{bmatrix}. \tag{11}
$$

The number of the required differential equations to describe the entire system is $6+n$, where n is the number of the DoF of the manipulator. Even though these equations are highly coupled, we can separate the second order terms forming the inertial matrix D, the gravitational terms forming the vector G, the coriolis terms for vector C and our inputs forming the τ vector as

$$
D(x)\ddot{x} + G(x) + C(x,\dot{x})\dot{x} = \tilde{\tau} + J^\top(x)F \tag{12}
$$

where $x = [x_t, y_t, z_t, \phi, \theta, \psi, \overline{q}]^\top$, $\overline{q} = [q_1, \ldots, q_n]^\top$, $(x_t, y_t, z_t)^\top$ are the coordinates of the Center of Mass of the UAV, $(\phi, \theta, \psi)^\top$ are the roll, pich and yaw angles of the UAV, and q_i the joint coordinate of the ith-joint of the manipulator. The structure of the $D_{(6+n)\times(6+n)}$ matrix is

$$
D = \left[\begin{array}{c|c|c} \left(m_s + \sum_{i=1}^{2} m_i\right) I_{3\times3} & M_{3\times3} & D^{RQ}_{6\times n}(x) \\ \hline [M]^\top & J^q_{3\times3} & \\ \hline & & \\ \left[D^{RQ}(x)\right]^\top & & D^{RR}_{n\times n}(\overline{q}) \end{array}\right]. \tag{13}
$$

Under the assumption that the gravity-vector is along the negative z-axis, the gravity vector can be written as $G = g\,[O_{1\times2}, G_3, G_4, \ldots, G_{6+n}]^\top$, where $G_i(x)$ with $i \in \{3, \ldots, 6+n\}$ depends on the configuration of both UAV and the manipulator.

Table 2. D Matrix Parameters

$M_{3\times3}$	System's Center of Mass Displacement
$J^q_{3\times3}$	System's Moment of Inertia
$D^{RQ}_{6\times n}(x)$	Manipulator-Quadrotor Interaction Matrix
$D^{RR}_{n\times n}(q)$	Manipulator Dynamic Inertia Matrix

The matrix $C_{(6+n)\times(6+n)}$ is the Coriolis and centrifugal vector and it accommodates the terms related with the linear and the angular velocities of the system.

The input vector $\tilde{\tau}$ can be written as $\tilde{\tau} = Bu$, where

$$B(\phi,\theta,\psi) = \left[\begin{array}{cccc|c} \cos\varphi\,\cos\psi\,\sin\vartheta + \sin\varphi\,\sin\psi & 0 & 0 & 0 & \\ \cos\varphi\,\sin\psi\,\sin\vartheta - \sin\varphi\,\cos\psi & 0 & 0 & 0 & \\ \cos\varphi\,\cos\vartheta & 0 & 0 & 0 & \\ 0 & la & 0 & 0 & O_{6\times n} \\ 0 & 0 & la & 0 & \\ 0 & 0 & 0 & 1 & \\ \hline \multicolumn{4}{c|}{O_{n\times 4}} & I_{n\times n} \end{array}\right],$$

$u = [U_1, \ldots, U_4, \tau]^\top$. Through separation of the external forces, J-Jacobian matrix can be computed as

$$J = \left[\, J^Q(x)_{6\times6} \left| \left[\begin{array}{c|c} {}^BR_2 & O_{3\times3} \\ O_{3\times3} & {}^BR_2 \end{array}\right] J^R(q)_{6\times n} \right]_{6\times(6+n)} \quad (14)$$

where the $J^R(q)$ is the Jacobian matrix of a fixed-base manipulator under the assumption that the UAV hovers.

The F-Force vector refers to the reaction forces upon the tip of the manipulator and is defined as $F = [F_x, F_y, F_z, \tau_x, \tau_y, \tau_z]^\top$, where F_i is the force at ith axis while τ_i is the torque about ith axis measured in the frame of the last link of the manipulator.

3. CONTROL DESIGN

The developed control strategy, shown in Fig. 2 considers the influence of each subsystem (UAV/manipultator) to the other. The proposed control strategy consists of: a) a controller for the manipulator designed to track the reference trajectory by using a feedback linearization technique, and b) a controller for the UAV that computes the desired states of the UAV, in order to follow a desired trajectory with respect to the E-frame.

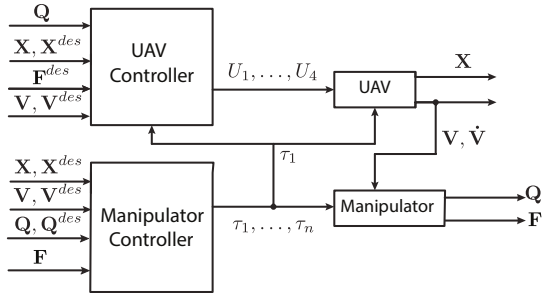

$\mathbf{X} = [x \quad y \quad z \quad \phi \quad \theta \quad \psi]^\top$
$\mathbf{V} = [V_E \quad \omega_B]^\top$
$\mathbf{Q} = [q_1 \quad \ldots \quad q_n \quad \dot{q}_1 \quad \ldots \quad \dot{q}_n]^\top$
$\mathbf{F} = [F_x \quad F_y \quad F_z \quad \tau_x \quad \tau_y \quad \tau_z]^\top$

Fig. 2. Controller framework

3.1 UAV-subsystem controller

The main idea is to account the nonzero values of UAV's roll and pitch depending on the direction of the forces that are to be applied at the tip by the manipulator. Thus, we compute the desired attitude for the UAV, so that the thrust generated by the UAV is able to nullify the external forces acting on the UAV. The thrust generated by the UAV's actuator is

$$F_z = U_1\ \cos\phi\ \cos\theta - m_t\ g \quad (15)$$
$$F_y = U_1\ \sin\phi \quad (16)$$
$$F_x = U_1\ \cos\phi\ \sin\theta. \quad (17)$$

with $m_t = m_s + \sum_{i=1}^{n} m_i$. Thus, given a desired force F^{des}, we are able to define the ϕ^{des} and θ^{des} by solving the equations (15-17) Having computed the desired attitude, a PD-controller is designed as

$$U_1 = \frac{m_t}{c\phi c\theta}\left(g - k_{d,z}\left(\dot{z} - \dot{z}^{des}\right) - k_{p,z}\left(z - z^{des}\right)\right)$$
$$U_2 = \frac{I_{xx}}{l_a}\left(-k_{d,\phi}\left(\dot{\phi} - \dot{\phi}^{des}\right) - k_{p,\phi}\left(\phi - \phi^{des}\right)\right)$$
$$U_3 = \frac{I_{yy}}{l_a}\left(-k_{d,\theta}\left(\dot{\theta} - \dot{\theta}^{des}\right) - k_{p,\theta}\left(\theta - \theta^{des}\right)\right)$$
$$U_4 = I_{zz}\left(-k_{d,\psi}\left(\dot{\psi} - \dot{\psi}^{des}\right) - k_{p,\psi}\left(\psi - \psi^{des}\right)\right)$$

In order to achieve positioning control in the $x-y$ -plane these equations are augmented to compensate the reaction torque τ_1 exerted by the manipulator, as

$$\bar{U}_1 = U_1 \quad (18)$$
$$\bar{U}_2 = U_2 + \nu_y\cos\psi - \nu_x\sin\psi + \tilde{\tau}_{1,x} \quad (19)$$
$$\bar{U}_3 = U_3 - \nu_x\cos\psi - \nu_y\sin\psi +]\tilde{\tau}_{1,y} \quad (20)$$
$$\bar{U}_4 = U_4 + \tilde{\tau}_{1,z},\ \text{where} \quad (21)$$

$$\nu_x = k_{d,x}\left(\dot{x} - \dot{x}^{des}\right) + k_{p,x}\left(x - x^{des}\right)$$
$$\nu_y = k_{d,y}\left(\dot{y} - \dot{y}^{des}\right) + k_{p,y}\left(y - y^{des}\right).$$
$$\begin{bmatrix}\tilde{\tau}_{1,x}\\ \tilde{\tau}_{1,y}\\ \tilde{\tau}_{1,z}\end{bmatrix} = \tau_1 \begin{bmatrix}1/la & 0 & 0\\ 0 & 1/la & 0\\ 0 & 0 & 1\end{bmatrix} {}^BR_O \begin{bmatrix}0\\0\\1\end{bmatrix}.$$

Additionally, this controller should cancel out the forces exerted on the UAV due to the interaction with its environment in order to stabilize and minimize the steady-state error of the UAV. Thus, the term $J(x)^\top F$ should be subtracted from the precomputed torques.

Furthermore, the movement of tee manipulator results in its center of mass not aligned with the center of the UAV. Hence, the counteracting torque on the UAV should be applied by adjusting terms U_2 and U_3.

3.2 Manipulator-subsystem controller

The employed controller consists of a classical computed torque controller augmented by the necessary force-term cancellation, as

$$\tau = \begin{bmatrix} C_{6+1}(x,\dot{x}) \\ \vdots \\ C_{6+n}(x,\dot{x}) \end{bmatrix} \dot{x} + \begin{bmatrix} G_{6+1}(x) \\ \vdots \\ G_{6+n}(x) \end{bmatrix} - (J^R(q))^\top F$$
$$- D^{RR}(q)\left(-\ddot{q}^{des} + K_d\left(\dot{q} - \dot{q}^{des}\right) + K_p\left(q - q^{des}\right)\right)$$

where K_p, K_d are positive (diagonal) matrices whose eigenvalues account for the transient response of the angle error and angular velocity error.

4. SIMULATION STUDIES

The efficiency of the suggested control schme was applied in simulation studies in an 'AscTec Pelican' quadrotor UAV with a planar two DoF attached as shown in Fig. 3. The implemented conrtoller was tested in a physics engine (Gazebo) simulation environment (Furrer et al., 2016).

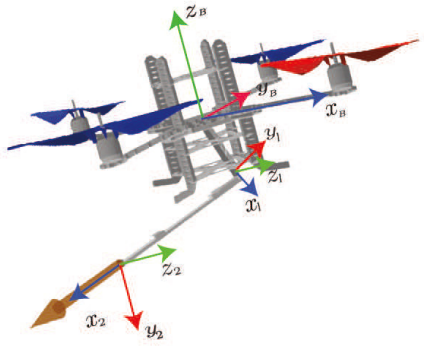

Fig. 3. UAV with attached manipulator and external forces

Table 3 lists the UAV and manipulator parameters.

Table 3. UAV/Manipulator Parameters

I_{xx}	0.01	$[kg \cdot m^2]$
I_{yy}	0.01	$[kg \cdot m^2]$
I_{zz}	0.02	$[kg \cdot m^2]$
m_s	1	$[kg]$
l_a	0.21	$[m]$
m_1	0.1	$[kg]$
l_1	0.1	$[m]]$
I_1	0.02	$[kg \cdot m^2]$
m_2	0.1	$[kg]$
l_2	0.3	$[m]$
I_2	0.02	$[kg \cdot m^2]$

To assess our control policy, three different scenarios were examined. In the first (second) scenario, the force exerted by the manipulator was increasing linearly, at a rate of $2\frac{N}{\text{sec}}$ saturation at 5 (10)N. Finaly, in the third scenario the force was chosen as $F^{des} = 5 + 5 \cdot \sin(2\pi \cdot 0.4 \cdot t - \frac{\pi}{2})\ N$ In all scenarios, our system tries to maintain its desired position with the second link parallel to the ground. The direction of the force coincides with the frame of the last link of the manipulator as shown in Fig. 1, so that it can simulate a push-action. Due to the configuration of the UAV and the direction of the force, the position error on x- axis is negligible, and thus we only present the position error in the $y - z$ plane.

Although, the controller is able to handle forces at any direction, forces that need to be compensated by using the input U_4 which refers to rotation around the z axis of the $B-$frame are nullified with more effort. Thus, that type of forces should firstly be handled by changing the configuration of the manipulator, so that it can minimize the force on that direction, and then nullify that force using U_4 . In all scenarios, we present the exerted force and the magnitude of the positioning error in the y and z-axes, when the force reaction is neglected, or, accounted for. Typical poses of the UAV/manipulator system at time instants $t = 0, 2, 4, 6, 8$ seconds appear in Fig. 4 indicating the UAV's adjustment of the roll, pitch and yaw angles to account for the applied force, while remaining at a constant position.

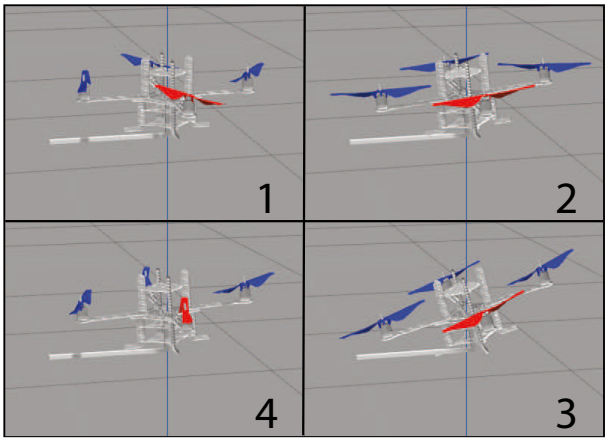

Fig. 4. UAV with attached manipulator in different poses

4.1 First simulation scenario

From the results presented in Figure 5, it is apparent that the positioning errors when the applied force is not compensated increase significantly (8× factor).

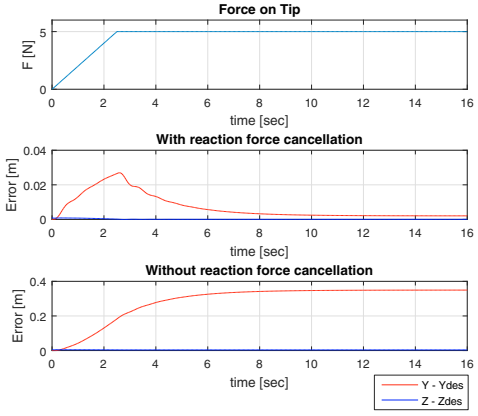

Fig. 5. First simulation study: System transient response

4.2 Second simulation scenario

From the system's transient response, shown in Figure 6, unless the applied force is compensated, the overall positioning error can be destabilized (after 14 seconds) resulting in an oscillatory response.

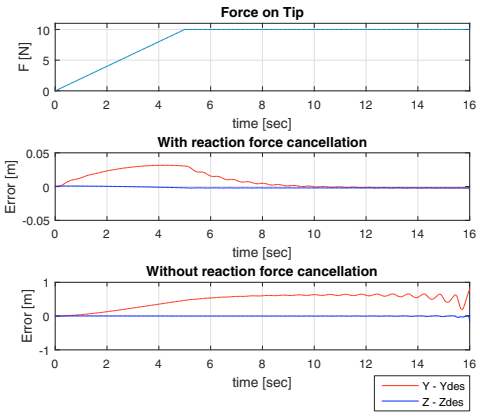

Fig. 6. Second simulation study: System transient response

4.3 Third simulation scenario

For the case of a sinusoidal appled force, from the obtained results shown in Figure 7, it is shown that for the compensated applied force case, when the initial position of the UAV is $(x, y, z) = (0, 0, 0.8)$ the UAV adjusts its altitude with a maximum positioning error of 0.05 m. For the uncompensated force case, the UAV oscillates at 0.5 m away from its desired position, as shown in Figure 8. The desired position is while a sequence of our system in the Gazebo Simulator is shown in Figure 4.

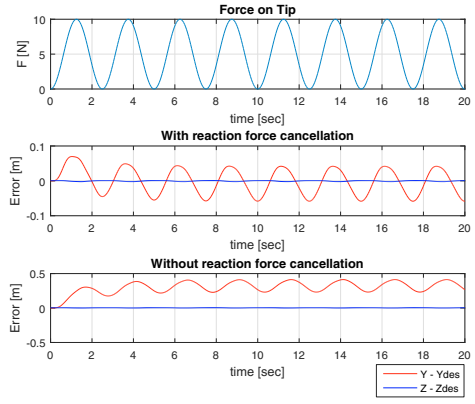

Fig. 7. Third simulation study: System transient response

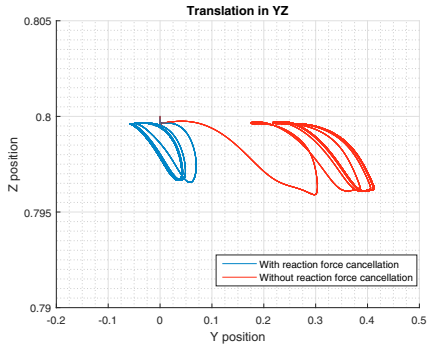

Fig. 8. UAV yz-plane transient position

5. CONCLUSIONS

This article concerns the modeling and control of a UAV with an attached manipulator applying a generalized force. The system's dynamic model is derived from the RNE method. The suggested distributed controller accounts for any interaction between the UAV and the manipulator subsystem. Simulation studies indicate the efficiency of the proposed controller and the need to compensate the applied force.

REFERENCES

Alexis, K., Nikolakopoulos, G., and Tzes, A. (2012). Model predictive quadrotor control: attitude, altitude and position experimental studies. *IET Control Theory & Applications*, 6(12), 1812–1827.

Fu, K., Gonzales, R., and Lee, C. (1987). Robotics: Control, sensing, vision, and intelligence. mcgrawhill. *Inc., Singapore*.

Furrer, F., Burri, M., Achtelik, M., and Siegwart, R. (2016). *Robot Operating System (ROS): The Complete Reference (Volume 1)*, chapter RotorS—A Modular Gazebo MAV Simulator Framework, 595–625. Springer International Publishing, Cham.

Kamel, M., Alexis, K., and Siegwart, R. (2016). Design and modeling of dexterous aerial manipulator. In *2016 IEEE/RSJ International Conference on Intelligent Robots and Systems (IROS)*, 4870–4876. doi: 10.1109/IROS.2016.7759715.

Marconi, L., Naldi, R., and Gentili, L. (2011). Modelling and control of a flying robot interacting with the environment. *Automatica*, 47(12), 2571–2583.

Pereira, P.O. and Dimarogonas, D.V. (2017). Stability of load lifting by a quadrotor under attitude control delay. In *2017 IEEE International Conference on Robotics and Automation (ICRA)*, 3287–3292. doi: 10.1109/ICRA.2017.7989374.

Pham, H.X., La, H.M., Feil-Seifer, D., and Deans, M. (2017). A distributed control framework for a team of unmanned aerial vehicles for dynamic wildfire tracking. In *2017 IEEE/RSJ International Conference on Intelligent Robots and Systems (IROS)*, 6648–6653. doi: 10.1109/IROS.2017.8206579.

Ruggiero, F., Lippiello, V., and Ollero, A. (2018). Aerial manipulation: A literature review. *IEEE Robotics and Automation Letters*, 3(3), 1957–1964.

Stergiopoulos, Y., Kontouras, E., Gkountas, K., Giannousakis, K., and Tzes, A. (2016). Modeling and control aspects of a uav with an attached manipulator. In *Control and Automation (MED), 2016 24th Mediterranean Conference on*, 653–658. IEEE.

Sujit, P.B., Saripalli, S., and Sousa, J.B. (2014). Unmanned aerial vehicle path following: A survey and analysis of algorithms for fixed-wing unmanned aerial vehicless. *IEEE Control Systems*, 34(1), 42–59. doi: 10.1109/MCS.2013.2287568.

Wopereis, H.W., Hoekstra, J.J., Post, T.H., Folkertsma, G.A., Stramigioli, S., and Fumagalli, M. (2017). Application of substantial and sustained force to vertical surfaces using a quadrotor. In *2017 IEEE International Conference on Robotics and Automation (ICRA)*, 2704–2709. doi:10.1109/ICRA.2017.7989314.